Thermal properties of $La_2Zr_2O_7$ double-layer thermal barrier coatings

Xingye Guo[a,b], Zhe Lu[c], Hye-Yeong Park[d], Li Li[e], James Knapp[e], Yeon-Gil Jung[d*], Jing Zhang[a**]

a. Department of Mechanical Engineering, Indiana University-Purdue University Indianapolis, IN 46202, USA

b. College of Materials Science and Engineering, Beijing University of Technology, Beijing, 100124, China

c. School of Materials and Metallurgical Engineering, University of Science and Technology Liaoning, Anshan, Liaoning Province, 114051, China

d. School of Materials Science and Engineering, Changwon National University, Changwon, Kyungnam 641-773, Republic of Korea

e Praxair Surface Technologies Inc., Indianapolis, IN 46222, USA

**Corresponding Authors:*jungyg@changwon.ac.kr; ** jz29@iupui.edu*

This is the author's manuscript of the article published in final edited form as:

Guo, X., Lu, Z., Park, H.-Y., Li, L., Knapp, J., Jung, Y.-G., & Zhang, J. (2018). Thermal properties of La2Zr2O7 double-layer thermal barrier coatings. Advances in Applied Ceramics, 0(0), 1–7. https://doi.org/10.1080/17436753.2018.1510820

Thermal properties of $La_2Zr_2O_7$ double-layer thermal barrier coatings

$La_2Zr_2O_7$ is a promising thermal barrier coating (TBC) material. In this work $La_2Zr_2O_7$ and 8YSZ layered TBC systems were fabricated. Thermal properties such as thermal conductivity and coefficient of thermal expansion were investigated. Furnace heat treatment and jet engine thermal shock (JETS) tests were also conducted. The thermal conductivities of porous $La_2Zr_2O_7$ single layer coatings are 0.50~0.66 W/m/^oC at the temperature range from 100 to 900 ^oC, which are 30~40% lower than the 8YSZ coatings. The coefficients of thermal expansion of $La_2Zr_2O_7$ coatings are about $9\sim10\times10^{-6}$ $^oC^{-1}$ at the temperature range from 200 ^oC to 1200 ^oC, which are close to those of 8YSZ at low temperature range and about 10% lower than 8YSZ at high temperature range. Double layer porous 8YSZ plus $La_2Zr_2O_7$ coatings show a better performance in thermal cycling experiments. It is likely because porous 8YSZ serves as a buffer layer to release stress.

Keywords: Thermal barrier coating; Lanthanum zirconate; Thermal cycling; Thermal conductivity; Coefficient of thermal expansion; Jet engine thermal shock

1. Introduction

Thermal barrier coatings (TBCs) are refractory-oxide ceramic coatings deposited to the surface of metallic parts in gas turbine engines, which include combustor, rotating blades, stationary guide vanes, blade outer air-seals, and afterburners in the tail section of jet engines, etc. TBCs are critical to gas turbine engines, since the gas temperatures are higher than the melting point of the metallic substrate parts [1-5]. TBCs provide high-temperature protection to the metallic substrate, which enable the gas-turbine engines to operate at significantly high temperatures. With the benefits of the high operation temperature, the energy efficiency of the gas turbines can be greatly increased. Typically commercial used TBCs are 7~8 wt% Y_2O_3 stabilized ZrO_2 (8YSZ) ceramics are deposited by air plasma-spraying (APS) or electron beam physical vapor deposition (EB-PVD). 8YSZ has a metastable tetragonal phase (*t'*). It transforms to tetragonal or cubic phases (*t* and *c*) when the temperature is above 1200 ºC, which will change the microstructure along with the mechanical properties [6]. As demanded by modern gas turbine engines, new TBCs suitable for operation above 1200 ºC need to be developed.

$La_2Zr_2O_7$ has been recently proposed as a promising TBC material. $La_2Zr_2O_7$ has no phase change from room temperature to its melting point, which is 2300 ºC. Compared with YSZ, it has a lower thermal conductivity (lower than 1.5W/m/K for $La_2Zr_2O_7$ and 2.1-2.2 for YSZ), lower sintering ability and lower coefficient of thermal expansion ($9.1\sim9.7\times10^{-6}$ K^{-1} for $La_2Zr_2O_7$ and $10.5\sim11.5\times10^{-6}$ K^{-1} for YSZ) [7]. Vassen *et al.* studied the thermal cycling behavior of single and double layered $La_2Zr_2O_7$ TBCs with the bottom layer of YSZ and top layer of $La_2Zr_2O_7$. The TBC systems were tested at the surface temperature between 1200 to 1450 ºC. The heating and cooling time periods were 5 minutes and 2 minutes, respectively. The results showed that the single-layer coatings had a rather poor thermal cycling performance and the double-layer systems showed similar results to YSZ coatings at the temperatures below about 1300 °C [8]. Yildirim *et al* studied the influence of temperature on phase stability and thermal conductivity of single- (SCL) and double-ceramic-layer (DCL) EB–PVD TBCs top coatings consisted of 7YSZ and $La_2Zr_2O_7$. The specific heat capacity and thermal conductivities of different compositions were measured [9]. Guo *et al.* reported the mechanical properties[10] and thermal cycling behavior [11-14] of 8YSZ and $La_2Zr_2O_7$ layered coatings. Jung *et al.* investigated the thermal cycling behavior of 8YSZ TBC

systems. The effects of the microstructure on the interfacial stability and fracture behavior of TBCs were investigated. The results revealed that the microstructural control is an important factor for stability, and it is necessary to optimize the porosity when the thick coatings are applied [15].

Although the mechanical properties of the $La_2Zr_2O_7$ coatings have been extensively studied, the thermal properties have not fully explored. The present study focuses on the thermal properties and thermal cycling behavior of layered $La_2Zr_2O_7$ coatings. The thermal conductivity and coefficient of thermal expansion of porous $La_2Zr_2O_7$ top coatings were studied. The thermal stability performance of both single and double layered TBCs was investigated using furnace heat treatment and jet engine thermal shock (JETS).

2. Experimental method

2.1 TBC sample preparation

The TBCs systems in this work include a metallic substrate, a metallic bond coating layer and one or two ceramic top coating layer. Haynes 188 superalloy was used as substrate in round button shape with the diameter of 1 inch and thickness of 0.125 inch. The bond coatings were deposited by APS technique using a Ni-based metallic feed stock powder, LN-65, with the thickness of 229 μm. All the top coatings were sprayed by APS using a Praxair patented plasma spray torch. Single layer commercial 8YSZ coatings and $La_2Zr_2O_7$ coatings were deposited with the same thickness and same porosities (11.54%). Two different types of double layer TBC systems were deposited: (1) porous 8YSZ coating + $La_2Zr_2O_7$ top coating, and (2) dense 8YSZ coating with vertical crack + $La_2Zr_2O_7$ top coating. Additionally, two single layer coatings, $La_2Zr_2O_7$ and porous 8YSZ, were fabricated for reference. The porosities of porous 8YSZ are in the same level as $La_2Zr_2O_7$ top coating. All type of samples are listed in Table 1. All of $La_2Zr_2O_7$ coating layers were sprayed using the same parameters. Additional coating samples preparation information is available in Ref. [11].

Table 1: 8YSZ and $La_2Zr_2O_7$ TBC samples

TBC type #	Top coatings	Thickness (μm)
1	$La_2Zr_2O_7$	432
2	Porous 8YSZ+ $La_2Zr_2O_7$	127+305
3	Dense 8YSZ + $La_2Zr_2O_7$	127+305
4	Porous 8YSZ	432

2.2 Experimental testing details

The porosity of the $La_2Zr_2O_7$ top coating was measured using free standing samples, which were peeled off from substrate without using a bond coating. The porosities were measured following the ASTM standard B328-94. The measurement device includes an analytical balance (Mettler AE240, Switzerland) and a density determination kit (Denver Instrument, density kit, Arvada, Colorado). Single layer $La_2Zr_2O_7$ samples with the thickness of 432 μm were used to measure the porosity and density. The measured average density and porosity are respectively 5.31g/cm^3 and 11.54%.

The thermal conductivities are calculated from thermal diffusivity $D_{th}(t)$, specific heat capacity $C_p(t)$ and measured density $\rho(t)$ [16]:

$$k = D_{th}(t) \cdot C_p(t) \cdot \rho(t) \quad (1)$$

Thermal diffusivities were measured by a flash diffusivity system (TA instrument DLF1200, Delaware). Coefficients of thermal expansion were measured by BAEHR dilatometer from room temperature to 1400 ºC.

Two thermal tests were conducted. The first one is the furnace thermal exposure test, which was conducted at 1080 ºC for 4 hours in argon atmosphere using round button samples with the diameter of 25.4 mm [17]. The second one is jet engine thermal shock (JETS) test, which is to investigate the thermal cycling performance with fast heating

and cooling cycles. The TBC samples were heated to 1232 ºC at the center for 20 s, and then cooled by compressed nitrogen cooling for 20 s and using ambient cooling for 40 s. This heating and cooling cycles repeated until the TBC samples failed. Both the front and back side temperatures were collected to investigate the temperature gradient.
The TBC samples were also sectioned and polished to conduct microstructural analysis according to ASTM-E1920-30. The cross-sectional microstructures were observed using a scanning electron microscope (SEM, JEOL Model JSM-5610, Japan).

3. Results and discussion

3.1 Thermal conductivity

Thermal conductivities were determined from the production of thermal diffusivity, specific heat capacity and density, as shown in Eq. 1. At selected temperatures (31ºC, 104 ºC, 306 ºC, 503 ºC, 701 ºC, and 901 ºC), at least three independent measurements were made. The average value of thermal diffusivity was used to calculate the thermal conductivity. The measured thermal conductivities and the fitting curves of porous $La_2Zr_2O_7$ and porous 8YSZ are plotted in Fig. 1. As shown in the figure, the thermal conductivities of $La_2Zr_2O_7$ coatings are about 30% lower than those of porous 8YSZ coatings.

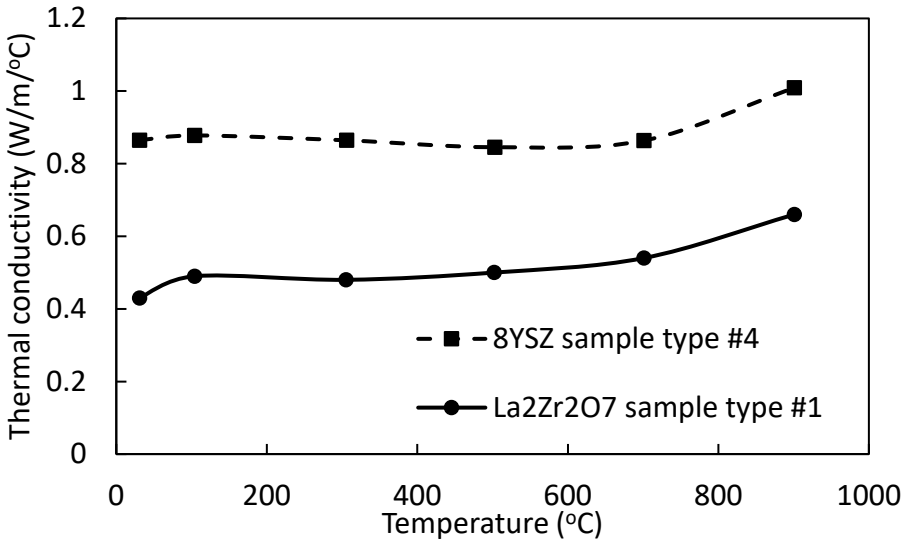

Fig. 1: Temperature dependent thermal conductivity of porous $La_2Zr_2O_7$ and porous 8YSZ coatings. Lines are for showing the trend.

There are a few guidelines that can be used to initially evaluate the thermal conductivity of TBC materials. Based on the assumption that the phonon mean free path approaches the mean inter-atomic distance, Clarke proposed the minimum thermal conductivity k_{min} in oxides [18]:

$$k_{\min} = 0.87 k_B \overline{\Omega}^{-2/3} (\frac{E}{\rho})^{1/2} \tag{2}$$

where $\overline{\Omega}$ is an effective atomic volume: $\overline{\Omega} = M/(m\rho N_A)$, where M is the mean atomic mass of the ions in the unit cell, m is the number of ions in the unit cell, ρ is the density, and E is Young's modulus. k_B and N_A are Boltzmann's constant and Avagadro's number, respectively.

To understand the systematic dependence of thermal conductivity, using kinetic theory of thermal transport, the thermal conductivity k is related to the mean free path λ by

$$k = \frac{1}{3} C_V \nu \lambda \tag{3}$$

where C_V is the specific heat, ν is the sound velocity, and λ is the mean free path [19].

For $La_2Zr_2O_7$, its mean free path is expected to be much shorter than 8YSZ, due to heavy rare earth element La serving as barriers to wave propagations. Therefore its thermal conductivity should be intrinsically less than that of 8YSZ.

The minimum thermal conductivity

3.2 Coefficient of thermal expansion

The temperature-dependent coefficients of thermal expansion of $La_2Zr_2O_7$ are shown in Fig. 2. The CTE values of $La_2Zr_2O_7$ are about $9\sim10\times10^{-6}$ $^oC^{-1}$ from 200 - 1200^{o}C, which are very close to the literature data. From Hayashi's experiment, 8YSZ coatings have CTE values of 9~10.9 $^oC^{-1}$ in same temperature range. So the CTE values of $La_2Zr_2O_7$ coatings are close to 8YSZ in the temperature range 200~500 ^{o}C, and about 10% lower than 8YSZ at temperatures above 500 ^{o}C. [7, 20].

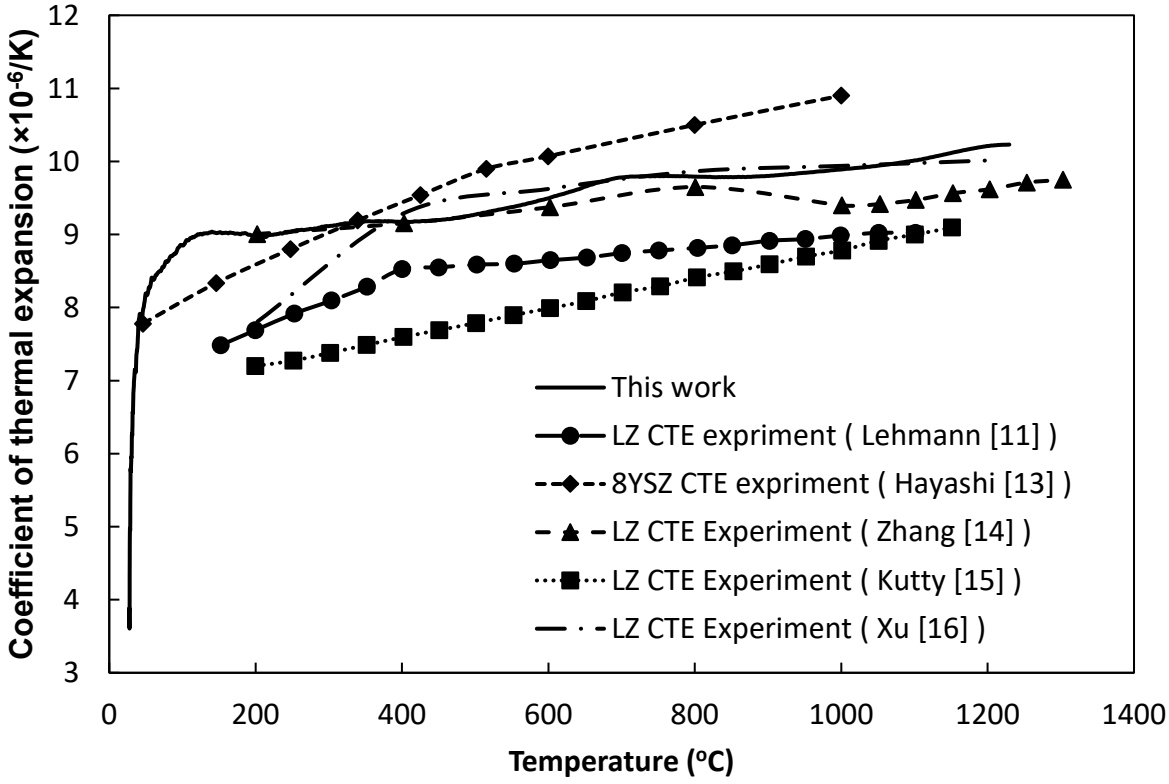

Fig. 2: Temperature-dependent CTE values of $La_2Zr_2O_7$, along with literature data of $La_2Zr_2O_7$ and 8YSZ [16, 20-23].

3.3 Furnace thermal exposure testing results

Fig. 3 shows the SEM images of cross-sectional microstructures of the 8YSZ and $La_2Zr_2O_7$ single and double layer coatings after the 4 hours of furnace thermal exposure. Except the single layer porous 8YSZ (Fig. 3d), all of the $La_2Zr_2O_7$ coatings were delaminated near the interface within $La_2Zr_2O_7$ region. This is mainly because the fracture toughness of $La_2Zr_2O_7$ coatings is low. Additionally, the discrepancy of thermal expansion coefficient between the top $La_2Zr_2O_7$ coating and beneath 8YSZ layer (Figs. 3b and 3c) or bond coating layer (Fig.3a) led to high thermal stress. The failure ultimately occurred due to the large residual stress near the interface within $La_2Zr_2O_7$ region [2].

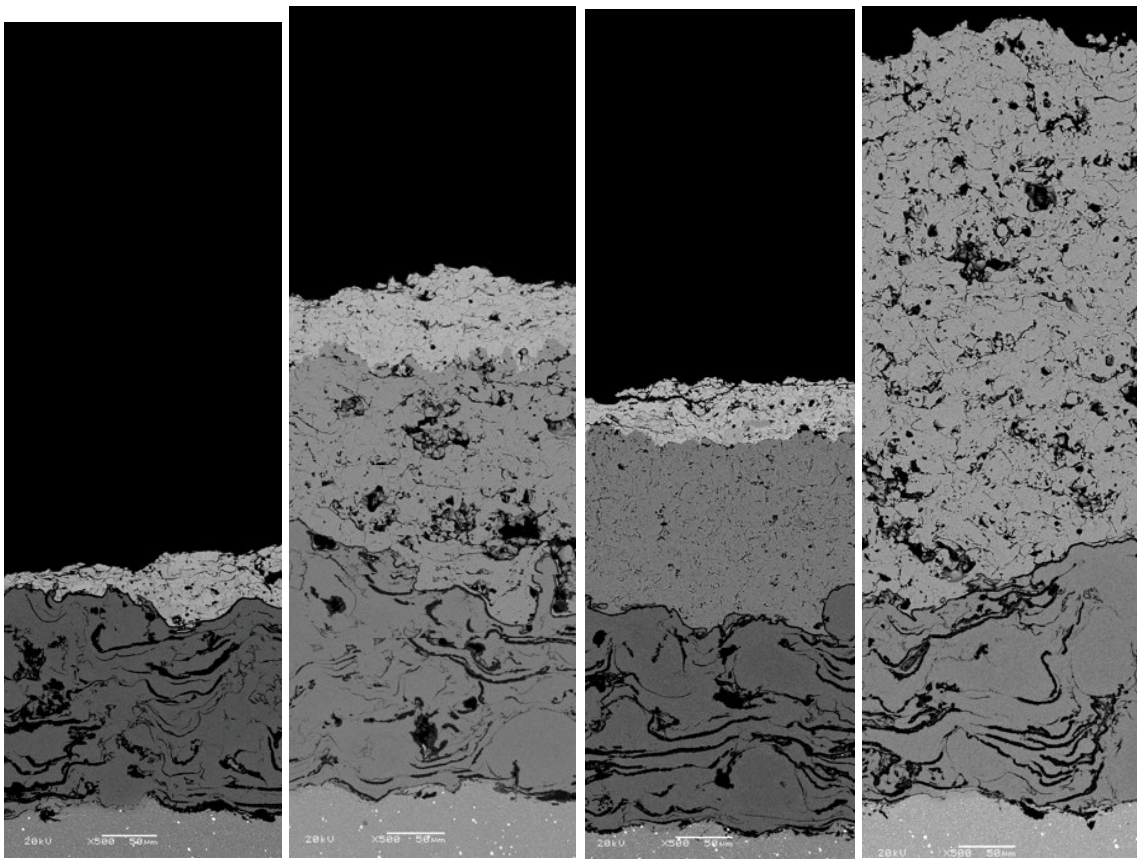

(a) (b) (c) (d)

Fig. 3: Microstructures of TBC samples after furnace thermal exposure test. (a) #1 porous $La_2Zr_2O_7$, (b) #2 $La_2Zr_2O_7$+ porous 8YSZ, (c) #3 $La_2Zr_2O_7$+ dense 8YSZ, and (d) #4 porous 8YSZ (scale bar is 50 μm)

Energy-dispersive X-ray spectroscopy (EDS) experiments were performed to check the diffusion tendency between the $La_2Zr_2O_7$ layer and 8YSZ layer. Only sample #2 $La_2Zr_2O_7$+ porous 8YSZ after 4 hours 1080 ºC thermal exposure was used in this analysis. As shown in Fig. 4, there is no obvious diffusion of Zr and La between two layers. So the diffusion effect can be excluded for this delamination of $La_2Zr_2O_7$. The thermal and mechanical properties of $La_2Zr_2O_7$ are the main reason to its failure.

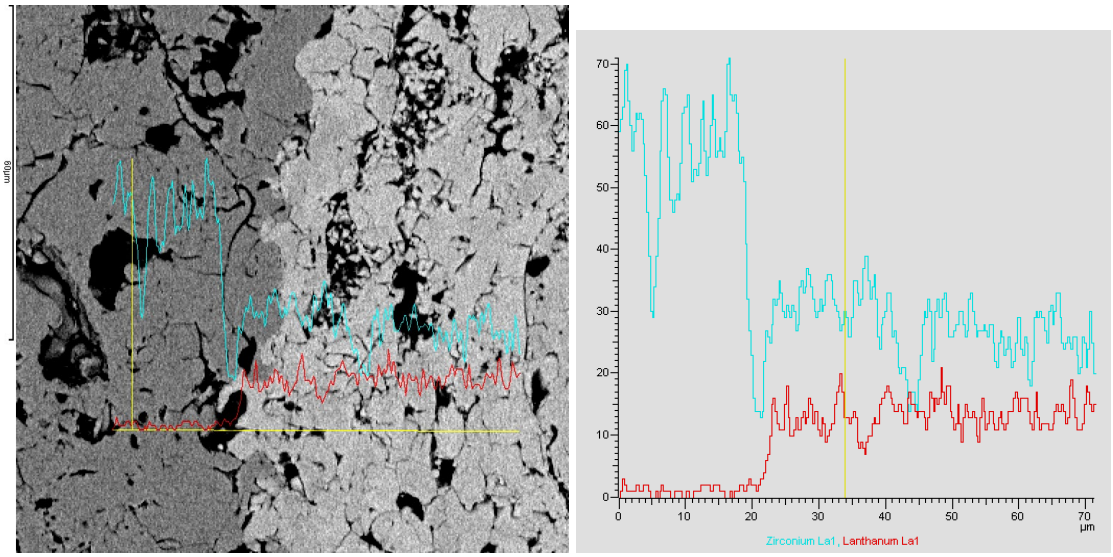

(a) (b)

Fig. 4: EDS analysis in the connection between La2Zr2O7 and 8YSZ coating layers in sample #2 $La_2Zr_2O_7$+ porous 8YSZ after thermal exposure test. (a) SEM image where the line of scan and EDS spectrum are overlaid, (b) intensity of Zr (blue) and La (red) elements.

3.4 Jet engine thermal shock testing results

For the JETS test, the round button TBC samples were heated to 1232 ^{o}C for 2000 cycles. All the single layer $La_2Zr_2O_7$ TBC samples were delaminated in the first 40 cycles. Similar to the furnace thermal exposure test, the delamination occurred at the interface between the bond coating and top coating layer. After 2000 cycles, the dense 8YSZ + $La_2Zr_2O_7$ coatings were completely delaminated. The delamination happened at the interface between the 8YSZ layer and $La_2Zr_2O_7$ top coating layer. However, the porous 8YSZ plus $La_2Zr_2O_7$ coatings were mainly intact. Only a few edges were cracked, about 60~70% $La_2Zr_2O_7$ top coating layer were still bonded with the porous 8YSZ layer. This porous 8YSZ plus $La_2Zr_2O_7$ coatings have much better thermal cycling performance than other $La_2Zr_2O_7$ coatings. All the 8 YSZ standard samples were intact after 2000 thermal shock cycles.

The single layer $La_2Zr_2O_7$ sample is shown in Fig. 5 (a). The coating was 100% delaminated from the bond coating layer. Only the bond coating and substrate left. This photo shows the rough interface of the connection area between bond coating and top coating. The JEST result of the dense 8YSZ and $La_2Zr_2O_7$ double layer coating is shown in Fig. 5 (c). After 2000 cycles JETS test, only the dense 8YSZ layer left on the substrate. The $La_2Zr_2O_7$ top coatings were totally lost after this thermal shock test. Delamination happened on the connection area of the 8YSZ and $La_2Zr_2O_7$ layer. Single layer 8YSZ coatings post-test samples are shown in Fig. 5 (d) as a standard sample. The top coatings of this TBC system are almost intact after 2000 cycles. The three black dents on the edge of the sample are the place where the clip located. There are no cracks on the surface of this 8YSZ top coating. It shows a significant higher lifetime.

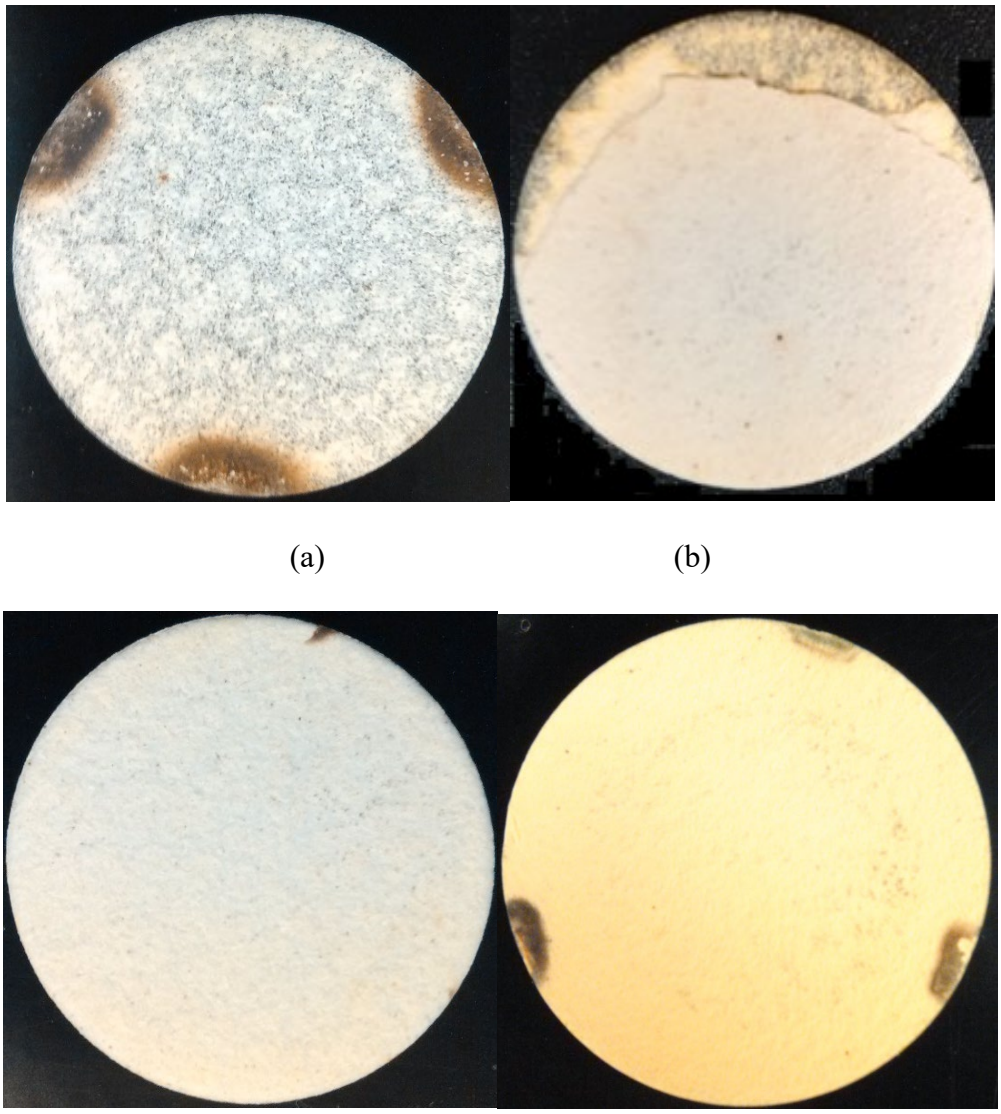

Fig. 5: Optical image of the JETS results after 2000 cycles. (a) #1 porous $La_2Zr_2O_7$, (b) #2 $La_2Zr_2O_7$+ porous 8YSZ, (c) #3 $La_2Zr_2O_7$+ dense 8YSZ, and (d) #4 porous 8YSZ

The porous 8YSZ and $La_2Zr_2O_7$ double layer coating's JEST result is shown in Fig. 5 (b). The $La_2Zr_2O_7$ top layer coatings have a few cracks on the edge. It did not delaminate in most part. The reason for this edge crack is probably related to the small radius of curvature at the outer rim. This type of double layer coatings shows a considerably better performance than the single layer $La_2Zr_2O_7$ coatings and dense 8YSZ+$La_2Zr_2O_7$ double layer coatings.

For round button samples, the heating and cooling of TBC systems will lead to residual thermal stress level in the ceramic topcoat perpendicular to the interface area. This residual stress level is proportional to distance from the interface. As a result, it will reduce linearly from the maximum value at the interface to zero at the free surface [6]. For this porous 8YSZ and La2Zr2O7 double layer system, the stress level at the interface of 8YSZ and $La_2Zr_2O_7$ is less than the stress level at the interface of 8YSZ and bond coating. The bond strength between 8YSZ and bond coating is much larger than the strength between $La_2Zr_2O_7$ and 8YSZ. However the residual stress at interface between 8 YSZ and $La_2Zr_2O_7$ is probably high enough to promote crack growth in this interface. So the $La_2Zr_2O_7$ coatings were delaminated by this residual stress. The interfaces of porous 8YSZ and $La_2Zr_2O_7$ coatings are much rougher than the interface between dense 8YSZ and $La_2Zr_2O_7$ shown in Fig. 6, because porous 8YSZ coatings have more cracks, pores and other defects in the interface, so porous 8YSZ and $La_2Zr_2O_7$ interfaces have higher bond strength than the dense one. In summary, it is probably because porous 8YSZ serves as a buffer layer to release stress.

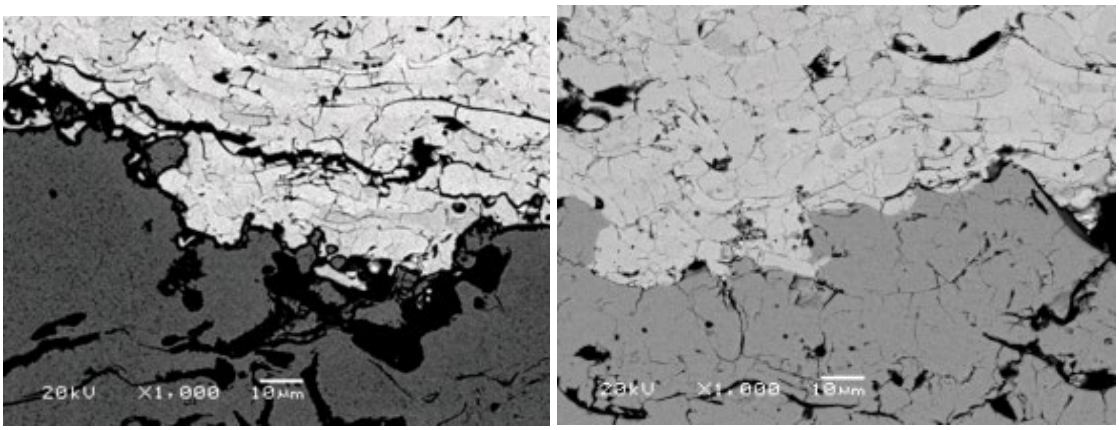

(a) (b)

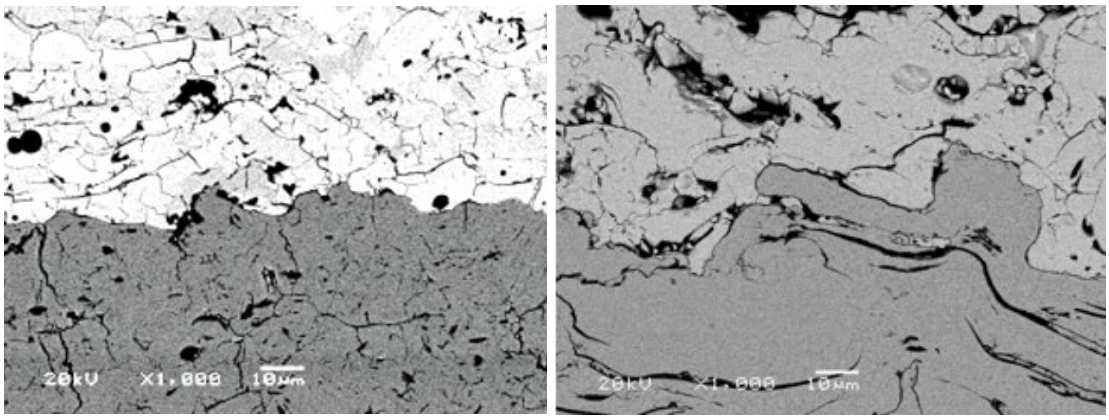

(c) (d)

Fig. 6: SEM images of coating interfaces between (a) $La_2Zr_2O_7$ and bond coating, (b) $La_2Zr_2O_7$ and porous 8YSZ, (c) $La_2Zr_2O_7$ and dense 8YSZ, and (d) porous 8YSZ and bond coating

Fig. 7 shows the temperature drop curves from the front to back surface of single layer $La_2Zr_2O_7$ and single layer porous 8YSZ samples. Both $La_2Zr_2O_7$ and 8YSZ coatings have 3 individual samples. Comparing with porous 8YSZ, the temperature drops in the $La_2Zr_2O_7$ top coating are about two times higher than the commercialized 8YSZ, because of the thermal conductivity of porous $La_2Zr_2O_7$ coatings are about 30% lower than 8YSZ coatings. But all of the porous $La_2Zr_2O_7$ coatings delaminated after 30 JETS cycles. The bond coatings and substrates were exposed to the JETS flame directly, so the temperature difference between front and back surface decreased severely. From Fig. 7, the temperature drops are only 200 ^oC.

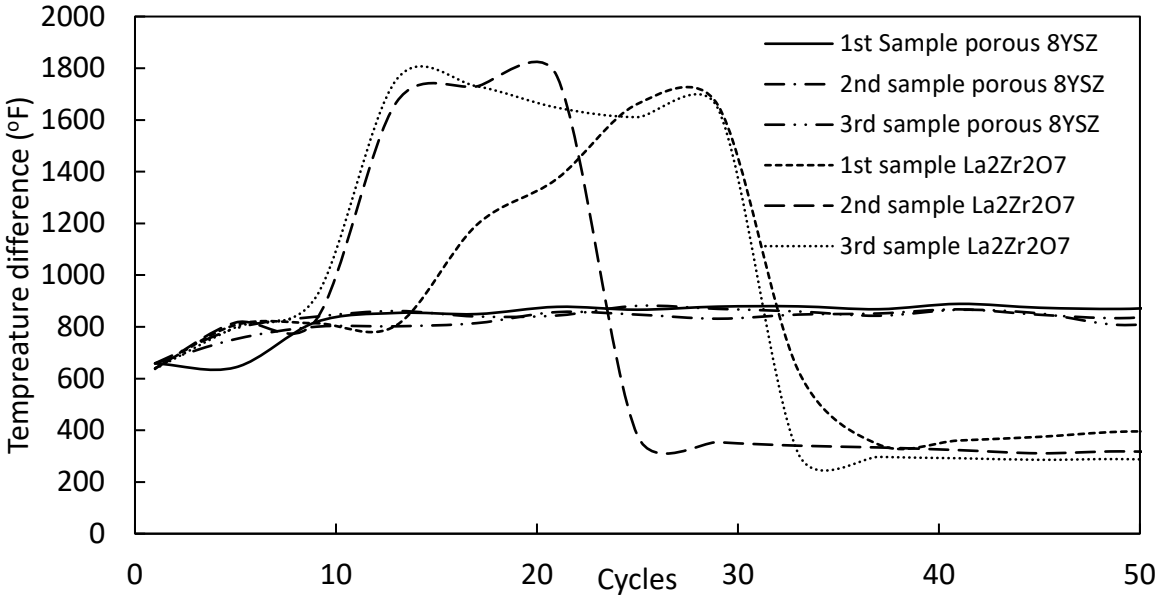

Fig. 7: Temperature difference between the front side and back side.

4. Conclusions

The thermal properties of $La_2Zr_2O_7$ and 8YSZ multilayer TBC systems were studied in this work. The major conclusions are summarized below.

1. All the $La_2Zr_2O_7$ coatings were delaminated in the 1080ºC heat treatment for 4 h. This is mainly because the low fracture toughness of $La_2Zr_2O_7$ material. The volume change due to the different CTE between bond coating layer and $La_2Zr_2O_7$ coating layer led to a high thermal stress. During the heating process, the inner thermal stresses were accumulated until the crack appeared.

2. The thermal conductivities of porous $La_2Zr_2O_7$ single layer coatings are 0.50~0.66 W/m/ºC at the temperature range from 100 ºC to 900 ºC, which are 30~40% lower than those of 8YSZ coatings.

3. The coefficients of thermal expansion of $La_2Zr_2O_7$ coatings are about $9\sim10\times10^{-6}$ ºC $^{-1}$ at the temperature range from 200 ºC to 1200 ºC, which are close to those of 8YSZ at low temperature range and about 10% lower than 8YSZ at high temperature range.

4. The double layer $La_2Zr_2O_7$ coatings with porous 8YSZ sublayer have better performance in the JETS test. It is probably because porous 8YSZ serves as a buffer layer to release stress.

5. Acknowledgement

J. Z. acknowledges the financial support provided by the United State Department of Energy (Grant No. DE-FE0008868, program manager: Richard Dunst) and Indiana University - Purdue University Indianapolis Research Support Funds Grant (RSFG) and International Research Development Fund (IRDF). Y.G.J acknowledges the financial support provided by "Human Resources Program in Energy Technology" of the Korea Institute of Energy Technology Evaluation and Planning (KETEP), granted financial resource from the Ministry of Trade, Industry & Energy, Republic of Korea. (No. 20174030201460). Z.L. acknowledges the financial support provided by the National Nature Science Foundation of China (Nos. 51702145).

References

[1] D. R. Clarke, M. Oechsner, and N. P. Padture, "Thermal-barrier coatings for more efficient gas-turbine engines," *MRS Bulletin,* vol. 37, pp. 891-898, 2012.

[2] A. G. Evans, D. R. Mumm, J. W. Hutchinson, G. H. Meier, and F. S. Pettit, "Mechanisms controlling the durability of thermal barrier coatings," *Progress in Materials Science,* vol. 46, pp. 505-553, 2001.

[3] D. Clarke and C. Levi, "Materials design for the next generation thermal barrier coatings," *Annual Review of Materials Research,* vol. 33, pp. 383-417, 2003.

[4] R. A. Miller, "Current status of thermal barrier coatings — An overview," *Surface and Coatings Technology,* vol. 30, pp. 1-11, 1987.

[5] R. Vaßen, M. O. Jarligo, T. Steinke, D. E. Mack, and D. Stöver, "Overview on advanced thermal barrier coatings," *Surface and Coatings Technology,* vol. 205, pp. 938-942, 11/15/ 2010.

[6] R. Vassen, X. Cao, F. Tietz, D. Basu, and D. Stöver, "Zirconates as New Materials for Thermal Barrier Coatings," *Journal of the American Ceramic Society,* vol. 83, pp. 2023-2028, 2000.

[7] X. Q. Cao, R. Vassen, and D. Stoever, "Ceramic materials for thermal barrier coatings," *Journal of the European Ceramic Society,* vol. 24, pp. 1-10, 2004.

[8] R. Vaßen, F. Traeger, and D. Stöver, "New Thermal Barrier Coatings Based on Pyrochlore/YSZ Double-Layer Systems," *International Journal of Applied Ceramic Technology,* vol. 1, pp. 351-361, 2004.

[9] K. Bobzin, N. Bagcivan, T. Brögelmann, and B. Yildirim, "Influence of temperature on phase stability and thermal conductivity of single- and double-ceramic-layer EB–PVD TBC top coats consisting of 7YSZ, $Gd_2Zr_2O_7$ and $La_2Zr_2O_7$," *Surface and Coatings Technology,* vol. 237, pp. 56-64, 12/25/ 2013.

[10] X. Guo, H.-M. Park, L. Li, J. Knapp, Y.-G. Jung, and J. Zhang, "Mechanical Properties of Layered La2Zr2O7 Thermal Barrier Coatings," *Journal of Thermal Spray Technology,* pp. https://doi.org/10.1007/s11666-018-0703-5 2018.

[11] X. Guo, Z. Lu, Y.-G. Jung, L. Li, J. Knapp, and J. Zhang, "Thermal Properties, Thermal Shock, and Thermal Cycling Behavior of Lanthanum Zirconate-Based Thermal Barrier Coatings," *Metallurgical and Materials Transactions E,* vol. 3, pp. 64-70, 2016.

[12] D. Song, U. Paik, X. Guo, J. Zhang, T.-K. Woo, Z. Lu*, et al.*, "Microstructure design for blended feedstock and its thermal durability in lanthanum zirconate based thermal barrier coatings," *Surface and Coatings Technology,* vol. 308, pp. 40-49, 2016.

[13] J. Zhang, X. Guo, Y.-G. Jung, L. Li, and J. Knapp, "Lanthanum Zirconate Based Thermal Barrier Coatings: A Review," *Surface and Coatings Technology,* 2016.

[14] J. Zhang and Y.-G. Jung, *Advanced Ceramic and Metallic Coating and Thin Film Materials for Energy and Environmental Applications*: Springer International Publishing, 2018.

[15] P.-H. Lee, S.-Y. Lee, J.-Y. Kwon, S.-W. Myoung, J.-H. Lee, Y.-G. Jung*, et al.*, "Thermal cycling behavior and interfacial stability in thick thermal barrier coatings," *Surface and Coatings Technology,* vol. 205, pp. 1250-1255, 11/25/ 2010.

[16] H. Lehmann, D. Pitzer, G. Pracht, R. Vassen, and D. Stöver, "Thermal Conductivity and Thermal Expansion Coefficients of the Lanthanum Rare-Earth-Element Zirconate System," *Journal of the American Ceramic Society,* vol. 86, pp. 1338-1344, 2003.

[17] B. Baufeld, M. Bartsch, and M. Heinzelmann, "Advanced thermal gradient mechanical fatigue testing of CMSX-4 with an oxidation protection coating," *International Journal of Fatigue,* vol. 30, pp. 219-225, 2008/02/01/ 2008.
[18] M. R. Winter and D. R. Clarke, "Oxide Materials with Low Thermal Conductivity," *Journal of the American Ceramic Society,* vol. 90, pp. 533-540, 2007.
[19] P. K. Schelling , S. R. Phillpot , and R. W. Grimes, "Optimum pyrochlore compositions for low thermal conductivity," *Philosophical Magazine Letters,* vol. 84, pp. 127-137, 2004/02/01 2004.
[20] H. Hayashi, T. Saitou, N. Maruyama, H. Inaba, K. Kawamura, and M. Mori, "Thermal expansion coefficient of yttria stabilized zirconia for various yttria contents," *Solid State Ionics,* vol. 176, pp. 613-619, 2/14/ 2005.
[21] J. Zhang, J. Yu, X. Cheng, and S. Hou, "Thermal expansion and solubility limits of cerium-doped lanthanum zirconates," *Journal of Alloys and Compounds,* vol. 525, pp. 78-81, 6/5/ 2012.
[22] K. V. G. Kutty, S. Rajagopalan, C. K. Mathews, and U. V. Varadaraju, "Thermal expansion behaviour of some rare earth oxide pyrochlores," *Materials Research Bulletin,* vol. 29, pp. 759-766, 7// 1994.
[23] C. Xu, C. Wang, C. Chan, and K. Ho, "Theory of the thermal expansion of Si and diamond," *Physical Review B,* vol. 43, pp. 5024-5027, 1991.